Second-order Raman spectra of diamond from *ab initio* phonon calculations

W. Windl, P. Pavone, K. Karch, O. Schütt, and D. Strauch
Institut für Theoretische Physik der Universität Regensburg, Universitätsstrasse 31, D-8400 Regensburg, Germany

P. Giannozzi
Scuola Normale Superiore, Piazza dei Cavalieri 7, I-56100 Pisa, Italy

S. Baroni
Scuola Internazionale Superiore di Studi Avanzati-International School for Advanced Studies (SISSA-ISAS), via Beirut 4, I-34014 Trieste, Italy

(Received 16 March 1993)

The second-order Raman spectra of diamond and silicon have been calculated using *ab initio* phonons and phenomenological polarizability coefficients. The sharp peak in the spectrum of diamond near the two-phonon cutoff is explained by a maximum in the vibrational density of states; this maximum originates from the uppermost phonon branch whose frequencies are calculated to have a minimum at the Brillouin-zone center. This frequency minimum as well as the sharp Raman peak are unique to diamond and do not occur for the other group-IV semiconductors. In our calculation based on harmonic *ab initio* lattice dynamics neither two-phonon bound states nor polarizability matrix element effects are needed to explain the peak, and we feel that the longstanding controversy about its origin has been resolved.

I. INTRODUCTION

One of the most interesting features in the two-phonon Raman spectrum of diamond is the sharp peak near the high-frequency cutoff, first noted by Krishnan[1] in 1946. Later Raman-scattering experiments have confirmed that this sharp peak occurs at[2] 2669 cm^{-1} (or[3] 2667 cm^{-1}) at room temperature, approximately 3 cm^{-1} (2 cm^{-1}) higher than twice the frequency of the first-order Raman line. For a short review, see Ref. 4.

First suggestions of attributing the sharp peak to two successive first-order Raman scatterings by Loudon[5] with subsequent calculations by Dolling and Cowley[6,7] have been shown to be unlikely by the investigations of Solin and Ramdas.[3]

Cohen, Ruvalds, and co-workers[8] explained the line by the existence of a two-phonon bound state that only would occur in the case of positive fourth-order force constants in diamond.[9] However, Vanderbilt, Louie, and Cohen[10] have shown by means of local-density functional frozen phonon calculations that the fourth-order coupling constants are negative. This suggests that two-phonon bound states cannot form in diamond.

An alternative explanation was the conjecture by Musgrave and Pople,[11] and then again by Uchinokura, Sekine, and Matsuura,[12] who suggested that the maximum frequency occurs away from the Γ point with the Γ point being a fluted saddle point. The most detailed investigation on this proposal (overbending with a saddle point) has been carried through by Tubino and Birman,[13] who found that the phonon dispersion of diamond does not have its maximum at Γ, but rather somewhere along the [100] direction of the uppermost (LO) branch.[14] A Raman peak originating from the saddle-point van Hove singularity at Γ should then occur at exactly twice the Raman frequency ω_0. Also, they suggested that anharmonic corrections would account for its slight frequency shift. Recently Wang, Chan, and Ho[15] proposed an overbending of the LO branch, with the LO branch in their model having its minimum frequency at Γ. Thus, in their model the peak in the two phonon density of states is above $2\omega_0$.

Go, Bilz, and Cardona[16] explained the peak by an anomaly in the bond polarizability of diamond.[17] So they were able to produce a peak in their spectra, although they did not have a visible overbending in their phonon dispersion.

Thus, in view of the different theories on the sharp peak, there seems to be the need for a final explanation. In this paper we will show that it is naturally explained by the occurrence of a minimum of the LO frequencies at the Brillouin-zone center. Furthermore, we will report on the Raman spectrum of silicon in order to discuss the differences between the diamond spectrum and the spectra of the "normal" group-IV semiconductors.

The structure of the paper is the following: At the beginning we summarize the common theory of two-phonon Raman scattering (Sec. II); then, we discuss the *ab initio* lattice dynamics on which the calculation of the Raman spectra is based (Sec. III) and our model for the second-order polarizability (Sec. IV). Finally, we show our results (Sec. V), discuss them (Sec. VI), and give a summary (Sec. VII).

II. THEORY OF TWO-PHONON RAMAN SCATTERING

Raman scattering of light by lattice vibrations of a crystal depends on the modulation of the electronic susceptibility χ by phonons (see, e.g., Ref. 5 or 18). Thus it is possible to separate the temporally fluctuating part $\delta\chi$ from the homogeneous χ_0:

$$\chi = \chi_0 + \delta\chi. \tag{1}$$

The fluctuating part of the susceptibility may be expanded in a power series in terms of the phonon coordinates:[18]

$$\delta\chi_{\alpha\beta} = P_{\alpha\beta} + \sum_j P_{\alpha\beta}(0j)\, A(0j) + \frac{1}{2}\sum_{\mathbf{q}jj'} P_{\alpha\beta}(\mathbf{q}jj')\, A(\mathbf{q}j)\, A(-\mathbf{q}j') + \cdots, \tag{2}$$

where the $A(\mathbf{q}j)$ are the sum of the phonon creation and destruction operators. The one-phonon contribution arises from the long-wavelength optic mode of vibration in the diamond structure. The coefficients of the two-phonon term, $P_{\alpha\beta}(\mathbf{q}jj')$, depend both on the wave vector $\mathbf{q}$ and the branch indices j and j'. Alternatively, $\delta\chi_{\alpha\beta}$ can be expressed as a power series in terms of phonon displacements, $\boldsymbol{u}\binom{l}{\kappa}$, where $\binom{l}{\kappa}$ indicates the κth sublattice in the lth unit cell,

$$\delta\chi_{\alpha\beta} = P_{\alpha\beta} + \sum_{l\kappa\gamma} P^{\gamma}_{\alpha\beta}\binom{l}{\kappa}\, u_\gamma\binom{l}{\kappa} + \frac{1}{2}\sum_{l\kappa l'\kappa'\gamma\delta} P^{\gamma\delta}_{\alpha\beta}\binom{l\ l'}{\kappa\ \kappa}\, u_\gamma\binom{l}{\kappa}\, u_\delta\binom{l'}{\kappa} + \cdots . \tag{3}$$

The displacements $\boldsymbol{u}\binom{l}{\kappa}$ can be expressed in terms of $A(\mathbf{q}j)$,

$$\boldsymbol{u}\binom{l}{\kappa} = \sum_{\mathbf{q}j}\sqrt{\frac{\hbar}{2\omega(\mathbf{q}j)NM_\kappa}}\,\boldsymbol{w}(\kappa|\mathbf{q}j)\, e^{i\mathbf{q}\cdot\mathbf{R}\binom{l}{\kappa}}\, A(\mathbf{q}j), \tag{4}$$

where $\boldsymbol{w}(\kappa|\mathbf{q}j)$ represents the eigenvectors of the normal modes and $\omega(\mathbf{q}j)$ their frequencies, while the vectors $\mathbf{R}\binom{l}{\kappa}$ indicate the atom sites. One gets for the second-order Raman polarizabilities from Eq. (2)

$$P_{\alpha\beta}(\mathbf{q}jj') = \frac{\hbar}{2\sqrt{\omega(\mathbf{q}j)\,\omega(\mathbf{q}j')}}\sum_{l\kappa\kappa'\gamma\delta} P^{\gamma\delta}_{\alpha\beta}\binom{0\ l}{\kappa\ \kappa'} \times w_\gamma(\kappa|\mathbf{q}j)\, w^*_\delta(\kappa'|\mathbf{q}j')\, e^{i\mathbf{q}\cdot\left[\mathbf{R}\binom{l}{\kappa'}-\mathbf{R}\binom{0}{\kappa}\right]}. \tag{5}$$

The scattering cross section depends upon the polarizations of the light and upon the crystal orientation. If the polarization of the electric vector of the incident light is defined by $\mathbf{e}^i$ and that of the scattered light by $\mathbf{e}^f$ the cross section is

$$\frac{d^2\sigma}{d\omega d\Omega} = \frac{1}{c_i c_f^3}\frac{\omega_f^2}{(2\pi\hbar)^2}\sum_{\alpha\beta\gamma\delta} e^i_\alpha\, e^f_\beta\, e^i_\gamma\, e^f_\delta\, I_{\alpha\beta\gamma\delta}(\omega), \tag{6}$$

where[18]

$$I_{\alpha\beta\gamma\delta}(\omega) = \frac{1}{2}\sum_{\mathbf{q}jj'} P_{\alpha\beta}(\mathbf{q}jj')\, P^*_{\gamma\delta}(\mathbf{q}jj') \times\delta[\omega(\mathbf{q}j)+\omega(\mathbf{q}j')-\omega] \tag{7}$$

represents the second-order Raman tensor at zero temperature.

III. *Ab initio* LATTICE DYNAMICS

The eigenvectors and eigenvalues that are necessary to evaluate Eq. (5) have been calculated using the local-density-approximation (LDA) plane-wave pseudopotential method of Baroni and co-workers.[19,20] An explicit description of the application of the method to diamond can be found in Ref. 21. The exchange-correlation energy has been taken from Ref. 22; the norm-conserving pseudopotentials have been constructed using the method of von Barth and Car.[23] The plane-wave basis has a cutoff energy of 16 Ry for silicon and 55 Ry for diamond. By using this plane-wave basis set the phonon dispersion has converged to within a relative deviation of less than 1%. For the summation in reciprocal space we have used ten Chadi-Cohen points.[24]

Natural diamond consists of the two isotopes ^{12}C (98.9%) and ^{13}C (1.1%). Besides the experimental Raman spectra[3] for natural diamond[25] (^{12}C) there are recent ones[26] for a nearly pure (96%) ^{13}C diamond. Therefore, we calculated the Raman spectra for both of them. Within the virtual-crystal approximation the force constants of diamond ^{13}C and ^{12}C are the same; thus, the frequencies are related by

$$\omega_{13}(\mathbf{q}j) = \sqrt{\frac{M_{12}}{M_{13}}}\,\omega_{12}(\mathbf{q}j). \tag{8}$$

Therefore, the frequencies for ^{13}C have been reduced by a factor of approximately 0.96 in comparison to those of ^{12}C.

The resulting phonon dispersion curves for diamond[21] ^{12}C and silicon[20] show two main differences: First, the flatness of the TA branches near the Brillouin zone boundaries that is characteristic of ZnS-structure semiconductors does not appear in the dispersion of diamond contrary to silicon; second, in diamond there is a strong overbending in the LO branch with a *minimum* at the Brillouin-zone center (Figs. 1 and 2). Because our main interest was focused on the sharp peak in the second-order Raman spectrum of diamond which will be shown to have its origin in the overbending (*vide infra*), we examined in particular this latter feature. The analysis of the force constants shows that an overbending of the LO branch in the phonon dispersion can be obtained only for significantly large values of the force constants between second neighbors.[21]

Because of the flatness of the TA branches in silicon,[20] its density of states is well structured in the acoustic region, whereas the density of states of diamond shows only some weak structures in this region (Fig. 3). Fur-

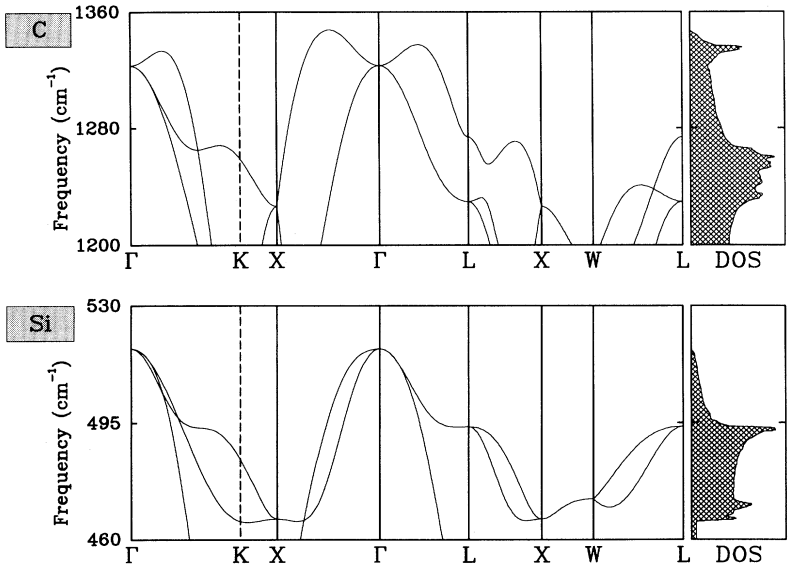

FIG. 1. High-frequency region of the *ab initio* phonon dispersion of diamond and silicon calculated with the corresponding interatomic force constants from Refs. 20 and 21. In contrast to silicon the top (LO) branch of diamond shows an overbending.

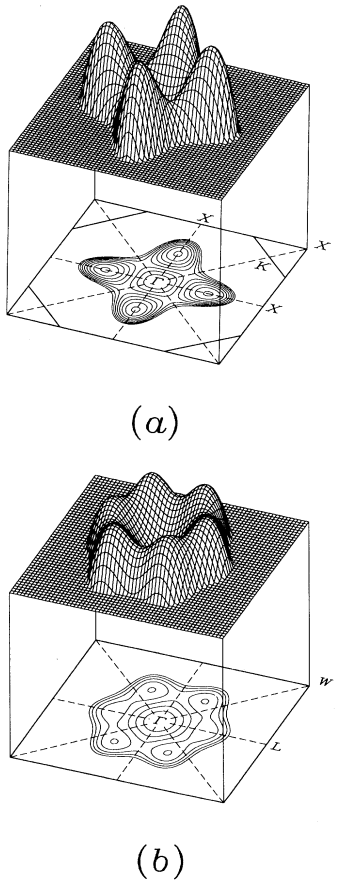

FIG. 2. Phonon dispersion sheet of diamond ^{12}C on (a) the (100) and (b) the (1$\bar{2}$1) plane. The zero level of the three-dimensional plot is the optical Γ point frequency; i.e., the displayed spectrum consists only of overbending frequencies. We also show the corresponding planes of the Brillouin zone with some special points and a contour plot of the phonon dispersion. The interval between contour lines is 3 cm^{-1}.

thermore, contrary to silicon we find a sharp peak at the frequency cutoff (at 1335.5 cm^{-1}) of the density of states of diamond slightly higher than $\omega_0 = 1323$ cm^{-1}. This is the result of an overbending of the LO branch with a minimum at the Γ point, whereas the maximum at the Brillouin-zone center in silicon results in no peak (an overbending with a saddle point at the Γ point would result in a peak at exactly ω_0).[27]

IV. MODEL FOR THE SECOND-ORDER POLARIZABILITY

There are 81 coefficients $P^{\gamma\delta}_{\alpha\beta}\binom{0\ l}{\kappa\ \kappa'}$ for each shell of neighbors that are partially related by symmetry prop-

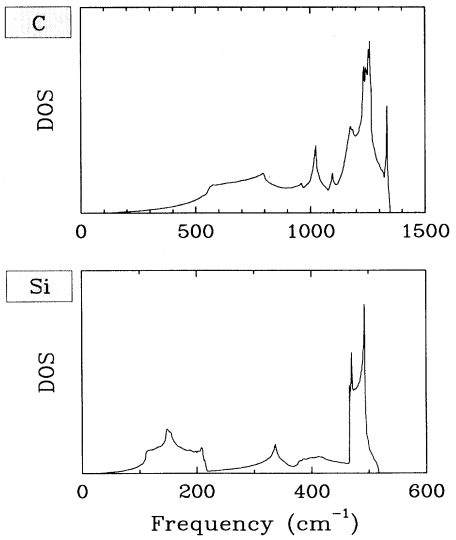

FIG. 3. Phonon density of states (DOS) of diamond ^{12}C and silicon from the phonon dispersions of Refs. 20 and 21 that have been calculated using the linear tetrahedron method (Ref. 34).

erties. Taking into account nearest-neighbor interaction and infinitesimal translational symmetry one is left with eight different coefficients. Using Voigt's notation and considering the neighbors at $\mathbf{R}\binom{0}{1} = (0,0,0)$ and $\mathbf{R}\binom{0}{2} = (1,1,1)\,a/4$, we get

$$P_I^J\left(\begin{smallmatrix}0&0\\1&2\end{smallmatrix}\right) = \left(\begin{array}{ccc|ccc} P_{11} & P_{12} & P_{12} & P_{14} & P_{15} & P_{15} \\ P_{12} & P_{11} & P_{12} & P_{15} & P_{14} & P_{15} \\ P_{12} & P_{12} & P_{11} & P_{15} & P_{15} & P_{14} \\ \hline P_{41} & P_{42} & P_{42} & P_{44} & P_{45} & P_{45} \\ P_{42} & P_{41} & P_{42} & P_{45} & P_{44} & P_{45} \\ P_{42} & P_{42} & P_{41} & P_{45} & P_{45} & P_{44} \end{array}\right). \quad (9)$$

Of the three representations of the Raman spectrum in the O_h point-group symmetry, the Γ_1^+ spectrum is expressed in terms of the parameters $P^1_{\Gamma_1^+} = P_{11} + 2P_{12}$ and $P^2_{\Gamma_1^+} = P_{14} + 2P_{15}$, the Γ_{12}^+ spectrum by the parameters $P^1_{\Gamma_{12}^+} = P_{11} - P_{12}$ and $P^2_{\Gamma_{12}^+} = P_{14} - P_{15}$, and the Γ_{25}^+ spectrum by the parameters P_{41}, P_{42}, P_{44}, and P_{45}.[28]

V. RESULTS

The results for the second-order Raman spectra for diamond ^{12}C, ^{13}C, and silicon are shown together with experimental curves[3,26,29] in Figs. 4–6. Best agreement of the theoretical spectra with the experimental ones was obtained with the parameters given in Table I.

In order to take into account linewidth and resolution effects, we have folded the calculated spectra with a Gaussian of the linewidth $\Delta\omega = 15.4$ cm^{-1}. In Table II and Table III we compare the experimental combination and overtone frequencies with our calculated values.

As shown in Table II and Fig. 4, for diamond ^{12}C we found—especially in comparison to previous work[6,16]—very good agreement between calculation and experiment (peak positions deviate by generally less than 2%). From Fig. 4 it can also be seen that within our harmonic approximation the sharp peak at the frequency cutoff in all the three representations is well reproduced as it should from symmetry considerations.[3,30] In fact, because of the low intensity of the Γ_{12}^+ and Γ_{25}^+ spectra (the relative intensities between the spectra of the three representations have been taken from Ref. 3), the experimental peak is not as clear as in the calculation because of noise. The calculated frequency of the sharp peak $\omega_{2\mathrm{Ra}}$ is slightly higher than twice the Raman frequency, $\omega_{2\mathrm{Ra}} - 2\omega_0 = 25$ cm^{-1} (see Table II). Because of the deviation of approximately 2% in our calculation, we could not reproduce the quantitative shift of 2 cm^{-1}; nevertheless, we can identify this sharp peak to be the projected sharp peak of the one-phonon density of states. Also the other peaks of the calculated spectrum are in good agreement with experiment in all three representations.

We also can confirm the existence of the two peaks at 1890 cm^{-1} and 2046 cm^{-1} which had been found experimentally in Ref. 3 and had not been definitely identified because of the very low intensity of the peaks and because of the absence of calculations in this region so far. In the acoustic region ($\omega \lesssim 1600$ cm^{-1}) we have found nearly zero intensity in agreement with experiment.[3]

There are recent experimental Raman spectra for diamond ^{13}C over the whole two-phonon frequency range.[26] The experimental curve together with the result of our calculation is shown in Fig. 5. The positions as well as the intensities of the maxima of the experimental curve and especially the sharp peak again can be reproduced very well by our calculation. The data confirm the fact that the scattered intensity is negligible in the low frequency region. Furthermore, the parameter ratios $P^2_{\Gamma_1^+}/P^1_{\Gamma_1^+}$ of ^{12}C and ^{13}C are the same (see Table I).

In order to show that the origin of the sharp peak at the high-frequency cutoff is not an effect of the matrix elements we also fitted the second-order Raman spectrum

TABLE I. Parameter relations giving the best agreement of the theoretical spectra with the experimental ones. We only report the parameters relative to each other because of the arbitrary units in all the experimental spectra.

Rel. Parameters	Diamond ^{12}C	Diamond ^{13}C	Silicon
$P^2_{\Gamma_1^+}/P^1_{\Gamma_1^+}$	−0.700	−0.704	−0.138
$P^2_{\Gamma_{12}^+}/P^1_{\Gamma_{12}^+}$	0.497		−0.401
P_{41}/P_{44}	−0.054		0.658
P_{42}/P_{44}	0.129		0.267
P_{45}/P_{44}	0.195		−0.214

TABLE II. Critical-point analysis of the second-order Raman spectra of diamond ^{12}C.

Overtones and Combinations	Active in	Theory (cm^{-1})	Experiment (cm^{-1})
"sharp peak"	$\Gamma_1^+, \Gamma_{12}^+, \Gamma_{25}^+$	2671	2670[a]
$2O(\Gamma)$	$\Gamma_1^+, \Gamma_{12}^+, \Gamma_{25}^+$	2646	2667[a]
$2L(X)$	$\Gamma_1^+, \Gamma_{12}^+, \Gamma_{25}^+$	2453	2370[b]
$2\mathrm{TO}(X)$	$\Gamma_1^+, \Gamma_{12}^+, \Gamma_{25}^+$	2186	2138[c]
$2\mathrm{TA}(X)$	$\Gamma_1^+, \Gamma_{12}^+, \Gamma_{25}^+$	1596	1614[c]
$L(X)+\mathrm{TA}(X)$	Γ_{25}^+	2024	1992[c]
$L(X)+\mathrm{TO}(X)$	Γ_{25}^+	2319	2254[b]
$\mathrm{TO}(X)+\mathrm{TA}(X)$	Γ_{12}^+	1891	1864[b]
$2O_2(W) = 2A_2(W)$	$\Gamma_1^+, \Gamma_{12}^+, \Gamma_{25}^+$	2035	1998[b]
$2O_1(W)$	$\Gamma_1^+, \Gamma_{12}^+, \Gamma_{25}^+$	2375	2358[c]
$2A_1(W)$	$\Gamma_1^+, \Gamma_{12}^+, \Gamma_{25}^+$	1864	1817[b]
$O_2(W) + O_1(W)$	$\Gamma_{12}^+, \Gamma_{25}^+$	2205	2177[b]
$A_2(W) + A_1(W)$	$\Gamma_{12}^+, \Gamma_{25}^+$	1949	1907[c]
$O_1(W) + A_1(W)$	$\Gamma_1^+, \Gamma_{12}^+, \Gamma_{25}^+$	2119	2178[c]
$2\mathrm{LO}(L)$	$\Gamma_1^+, \Gamma_{25}^+$	2548	2504[b]
$2\mathrm{TO}(L)$	$\Gamma_1^+, \Gamma_{12}^+, \Gamma_{25}^+$	2459	2422[b]
$2\mathrm{LA}(L)$	$\Gamma_1^+, \Gamma_{25}^+$	2147	2011[b]
$2\mathrm{TA}(L)$	$\Gamma_1^+, \Gamma_{12}^+, \Gamma_{25}^+$	1117	1126[c]
$\mathrm{LO}(L)+\mathrm{TO}(L)$	$\Gamma_{12}^+, \Gamma_{25}^+$	2503	2458[b]
$\mathrm{LA}(L)+\mathrm{TA}(L)$	$\Gamma_{12}^+, \Gamma_{25}^+$	1632	1569[c]

[a]Ref. 2.
[b]Ref. 3.
[c]Not experimentally found but calculated from Ref. 3.

in its three representations for silicon. The results of the calculations are shown in Fig. 6.

A comparison of combination and overtone frequencies is reported in Table III. Again we find good agreement between calculation and experiment for all representations. The positions of the calculated peaks agree with the experimental values within generally less than 2%. Especially the Γ_1^+ spectrum exhibits particularly strong structures in the acoustic frequency region up to 450 cm^{-1}. These are effects of the flatness of the TA branch; see the dispersion relation in Ref. 20 and the density of states in Fig. 3. As expected from the phonon dispersion and the high-frequency density of states (see Fig. 1) there is no sharp peak at the high-frequency cutoff.

VI. DISCUSSION

For all three spectra the similarity between the overtone density of states and the Γ_1^+ spectrum which is dominated by overtones[30] can clearly be seen. However, there are significant differences between the overtone densities of states (ODOS) and the corresponding Γ_1^+ spectra that point out the necessity of calculating the Raman spectra.

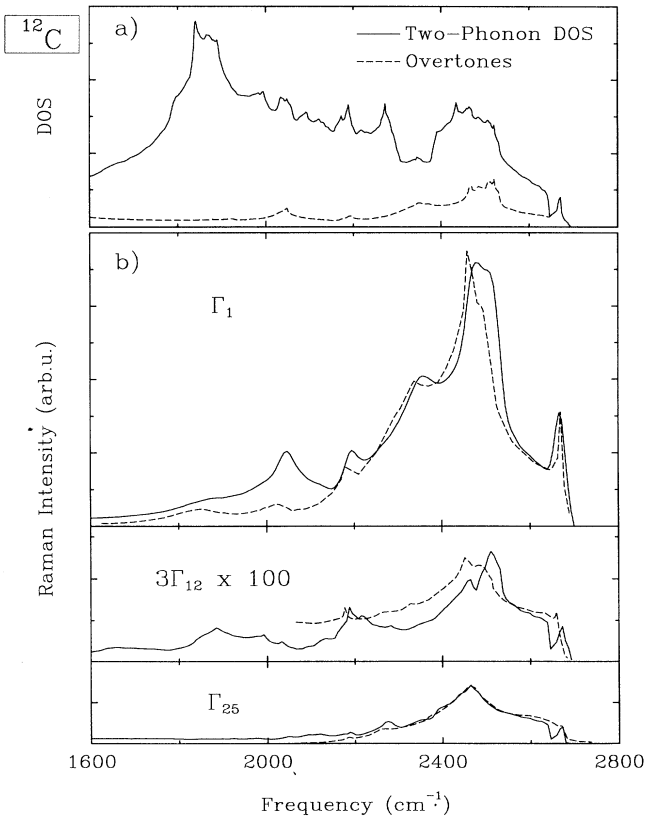

FIG. 4. (a) Two-phonon and overtone density of states of diamond ^{12}C. (b) Second-order Raman spectrum of diamond ^{12}C in the high-frequency region. The solid lines represent the calculated spectra; the dashed lines are experimental ones from Ref. 3.

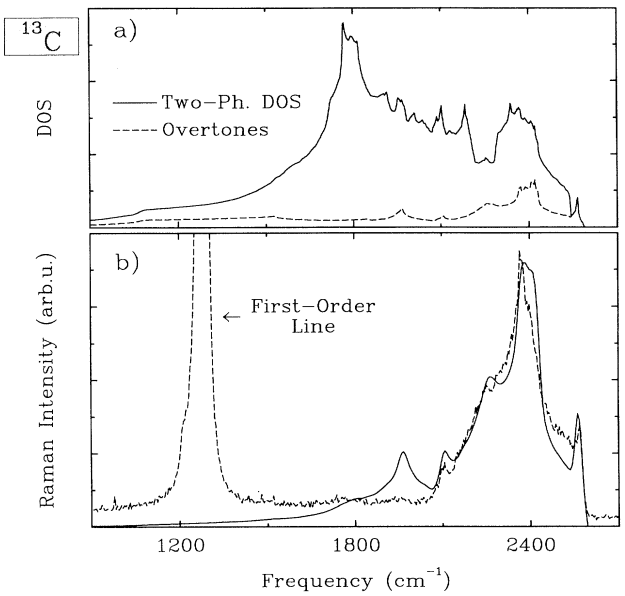

FIG. 5. (a) Two-phonon and overtone density of states of diamond ^{13}C. (b) Second-order Raman spectrum of diamond ^{13}C. The solid line represents the calculated Γ_1^+ spectrum; the dashed line is an experimental $(\Gamma_1^+ + \Gamma_{12}^+)$ spectrum from Ref. 26; because of the relatively low intensity of the Γ_{12}^+ spectrum (Ref. 3), this is a nearly pure Γ_1^+ spectrum.

First, the relative intensities of the ODOS and Γ_1^+ spectra differ significantly so that it is hard to tell only from the ODOS which peaks will appear in the Γ_1^+ spectrum and which ones will not (see, e.g., the nearly zero intensity in the low-frequency region of the Γ_1^+ spectra of diamond, Fig. 5). Second, in addition to the peaks that are expected from the ODOS new ones appear in the Raman spectrum (see, e.g., the peak slightly above 600 cm^{-1} in the Γ_1^+ spectrum of silicon, Fig. 6). Therefore, the ODOS must be looked upon rather as a low-order approximation of the Γ_1^+ Raman spectrum than as something that could reliably represent the features of the spectrum.

The Raman spectra for the two diamond isotopes as well as for silicon could be reproduced in better agreement with experiment than in previous work without invoking *ad hoc* assumptions as done in Ref. 16 and without the fortuitous model results of Ref. 13 as have been discussed in subsequent work.[31–33] Thus we believe that there is now a final explanation for the sharp peak in the second-order Raman spectrum of diamond.

Second-order Raman spectra are projected two-phonon densities of states, weighted with the matrix elements $P_{\alpha\beta}(\mathbf{q}jj')\,P^*_{\gamma\delta}(\mathbf{q}jj')$. They can be well evaluated in nearest-neighbor approximation as the latter reproduces experimental spectra very well. Changing the fitting parameters—i.e., the second derivatives of the polarizability with respect to the displacements—results in intensity changes of the various peaks of the two-phonon density of states, but does not create new peaks. Therefore the appearance of the "anomalous" peak in the second-order Raman spectrum of diamond is caused by nothing else but its "anomalous" density of states.

VII. SUMMARY

In this paper we have shown results for the second-order Raman spectra of diamond ^{12}C and ^{13}C and for silicon using *ab initio* force constants calculated by the method of Baroni and co-workers[19,20] and phenomenological matrix elements in the nearest-neighbor approximation. The spectra of diamond and silicon are different in two respects: Contrary to silicon diamond exhibits negligible scattering from acoustical-phonon combinations, but has a prominent peak at slightly more than twice the Raman frequency.

This peak, which is also found in the two-phonon density of states, results from a corresponding peak in the one-phonon density of states, which in turn is produced by LO phonons with frequencies higher than the Raman frequency. In fact, the LO branch has a *minimum* at the Brillouin-zone center, resulting in a peak *higher* than twice the Raman frequency; a saddle point would result in a peak *at* twice the Raman frequency and a maximum in *no* peak at all. Our LO frequency minimum is in contrast to previous model calculations which either result in a saddle point[13] or, in most cases, in a maximum. In Ref. 27 a minimum or a saddle point was artificially generated in order to demonstrate the above-described effects on the two-phonon Raman spectrum.

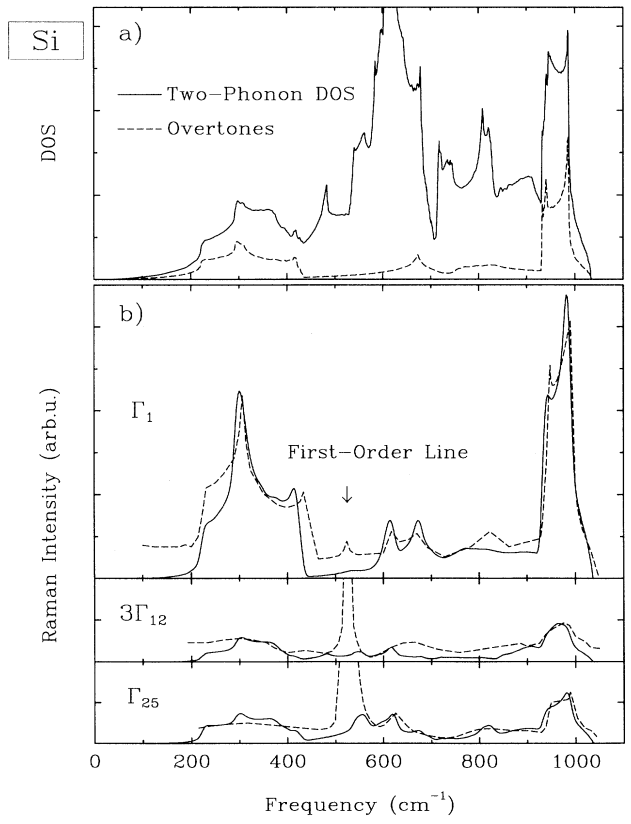

FIG. 6. (a) Two-phonon and overtone density of states of silicon. (b) Second-order Raman spectrum of silicon. The solid lines represent calculated spectra; the dashed lines are experimental ones from Ref. 29.

TABLE III. Critical-point analysis of the second-order Raman spectra of silicon.

Overtones and Combinations	Active in	Theory (cm^{-1})	Experiment (cm^{-1})
$2O(\Gamma)$	Γ_1^+, Γ_{12}^+, Γ_{25}^+	1034	1038[a]
$2L(X)$	Γ_1^+, Γ_{12}^+, Γ_{25}^+	828	825[b]
$2\mathrm{TO}(X)$	Γ_1^+, Γ_{12}^+, Γ_{25}^+	932	923[b]
$2\mathrm{TA}(X)$	Γ_1^+, Γ_{12}^+, Γ_{25}^+	290	299[b]
$L(X)+\mathrm{TA}(X)$	Γ_{25}^+	559	562[c]
$L(X)+\mathrm{TO}(X)$	Γ_{25}^+	880	874[c]
$\mathrm{TO}(X)+\mathrm{TA}(X)$	Γ_{12}^+	611	611[c]
$2O_2(W) = 2A_2(W)$	Γ_1^+, Γ_{12}^+, Γ_{25}^+	715	743[d]
$2O_1(W)$	Γ_1^+, Γ_{12}^+, Γ_{25}^+	945	948[b]
$2A_1(W)$	Γ_1^+, Γ_{12}^+, Γ_{25}^+	409	434[b]
$O_2(W)+O_1(W)$	Γ_{12}^+, Γ_{25}^+	830	845[c]
$A_2(W)+A_1(W)$	Γ_{12}^+, Γ_{25}^+	562	588[c]
$O_1(W)+A_1(W)$	Γ_1^+, Γ_{12}^+, Γ_{25}^+	677	691[c]
$2\mathrm{LO}(L)$	Γ_1^+, Γ_{25}^+	838	841[e]
$2\mathrm{TO}(L)$	Γ_1^+, Γ_{12}^+, Γ_{25}^+	988	983[b]
$2\mathrm{LA}(L)$	Γ_1^+, Γ_{25}^+	755	760[b]
$2\mathrm{TA}(L)$	Γ_1^+, Γ_{12}^+, Γ_{25}^+	220	226[a]
$\mathrm{LO}(L)+\mathrm{TO}(L)$	Γ_{12}^+, Γ_{25}^+	912	912[c]
$\mathrm{LA}(L)+\mathrm{TA}(L)$	Γ_{12}^+, Γ_{25}^+	488	493[c]

[a]Ref. 29.
[b]Ref. 12.
[c]Not experimentally found but calculated from experimental data.
[d]Infrared data from Ref. 35.
[e]Neutron data from Ref. 36.

The Raman spectra are essentially combination and overtone two-phonon densities of states weighted by polarizability coefficients. Restriction to nearest neighbors results in eight coefficients, two for each the Γ_1^+ and the Γ_{12}^+ spectrum and four for the Γ_{25}^+ spectrum. These can only be determined relative to each other because of the arbitrary units in all the experimental spectra. The parameter relations for diamond are equal for the Γ_1^+ spectra of the two isotopes ^{12}C and ^{13}C which implies a reliable calculation. Furthermore, the significant differences between the parameter sets of diamond and silicon show that the parameter ratios are different for various elements of the same crystal class. Inclusion of the second-neighbor parameters alters only the relative peak intensities, but does not change the qualitative appearance. Thus the peak at slightly more than twice the Raman frequency in the diamond Raman spectrum can be traced back to be a consequence of the anomalous phonon dispersion in that material.

There is no need to invoke matrix-element effects or two-phonon bound states. The long-standing controversy seems to be resolved.

A confirmation and maybe an improvement of this calculation which has employed phenomenological polarizability coefficients would be the use of *ab initio* polarizabilities. This will be taken up when first-principles coefficients are available. Otherwise, the Raman spectra of the group-IV elemental semiconductors now seem to be well understood.

ACKNOWLEDGMENTS

We like to thank Dr. E. Steigmeier from the Paul Scherrer Institut Zürich for communicating the ^{13}C spectra on a specimen supplied by Dr. W. F. Banholzer from the GE Corporate Research and Development. This work has been cosponsored by the Deutsche Forschungsgemeinschaft (Graduierten-Kolleg: Komplexität in Festkörpern) under Contract No. SCHR123/8.

[1] R. S. Krishnan, Proc. Indian Acad. Sci. A **24**, 45 (1946); **26**, 399 (1947).
[2] M. A. Washington and H. Z. Cummins, Phys. Rev. B **15**, 5840 (1977).
[3] S. A. Solin and A. K. Ramdas, Phys. Rev. B **1**, 1687 (1970).
[4] S. A. Solin, Phys. Rev. Lett. **53**, 2517 (1984).
[5] R. Loudon, Adv. Phys. **13**, 423 (1964).
[6] R. A. Cowley, J. Phys. (Paris) **26**, 659 (1965).
[7] G. Dolling and R. A. Cowley, Proc. Phys. Soc. London **88**, 463 (1966).
[8] M. H. Cohen and J. Ruvalds, Phys. Rev. Lett. **23**, 1378 (1969); and a lot of subsequent work, e.g., J. Ruvalds and A. Zawadowski, Phys. Rev. B **2**, 1172 (1970); J. Ruvalds, *ibid.* **10**, 3556 (1971); J. Ruvalds and A. Zawadowski, in *Light Scattering in Solids*, edited by M. Balkanski (Flammarion, Paris, 1971), p. 29.
[9] For compelling hints that the two-phonon bound states were no satisfactory explanation for the sharp peak, see, e.g., C. H. Wu and J. L. Birman, J. Phys. Chem. Solids **36**, 305 (1975).
[10] D. Vanderbilt, S. G. Louie, and M. L. Cohen, Phys. Rev. Lett. **53**, 1477 (1984).
[11] M. J. P. Musgrave and J. A. Pople, Proc. R. Soc. London A **268**, 474 (1962).
[12] K. Uchinokura, T. Sekine, and E. Matsuura, J. Phys. Chem. Solids **35**, 171 (1974).
[13] R. Tubino and J. L. Birman, Phys. Rev. B **15**, 5843 (1977).
[14] For the sake of simplicity we will call the uppermost phonon branch in the following LO branch, even if it is only for two main symmetry directions really longitudinal.
[15] C. Z. Wang, C. T. Chan, and K. M. Ho, Solid State Commun. **76**, 483 (1990).
[16] S. Go, H. Bilz, and M. Cardona, Phys. Rev. Lett. **34**, 580 (1975); S. Go, Ph.D. thesis, Universität Stuttgart, 1975.
[17] M. Cardona, in *Light Scattering in Solids II*, edited by M. Cardona and G. Günterrodt, Vol. 50 of *Topics in Applied Physics* (Springer, Berlin, 1982), p. 62.
[18] M. Born and K. Huang, *Dynamical Theory of Crystal Lattices* (Oxford University Press, Oxford, 1954).
[19] S. Baroni, P. Giannozzi, and A. Testa, Phys. Rev. Lett. **58**, 1861 (1987).
[20] P. Giannozzi, S. de Gironcoli, P. Pavone, and S. Baroni, Phys. Rev. B **43**, 7231 (1991).
[21] P. Pavone, K. Karch, O. Schütt, W. Windl, D. Strauch, P. Gianozzi, and S. Baroni, preceding paper, Phys. Rev. B **48**, 3156 (1993).
[22] J. Perdew and A. Zunger, Phys. Rev. B **23**, 5048 (1981).
[23] U. von Barth and R. Car (unpublished).
[24] D. J. Chadi and M. L. Cohen, Phys. Rev. B **8**, 5747 (1973).
[25] We have found by means of coherent potential approximation that the differences between the calculated phonons for natural diamond and pure ^{12}C diamond are negligible. The same holds for pure ^{13}C diamond and the experimentally examined specimen with 96% of the isotope ^{13}C. For this reason we write for natural diamond further on ^{12}C, for the other examined type of diamond ^{13}C.
[26] E. Steigmeier (private communication).
[27] K. C. Hass, M. A. Tamor, T. R. Anthony, and W. F. Banholzer, Phys. Rev. B **45**, 7171 (1992).
[28] H. Bilz, D. Strauch, and R. K. Wehner, *Handbuch der Physik, Bd. XXV/2d: Licht und Materie*, edited by S. Flügge (Springer, Berlin, 1984), p. 148.
[29] P. A. Temple and C. E. Hathaway, Phys. Rev. B **7**, 3685 (1973).
[30] J. L. Birman, Phys. Rev. **127**, 1093 (1962); **131**, 1489 (1963).
[31] A. D. Zdetsis, Solid State Commun. **34**, 199 (1980).
[32] W. Weber, Phys. Rev. B **15**, 4789 (1977).
[33] R. D. Turner and J. C. Inkson, J. Phys. C **11**, 3961 (1978).
[34] G. Lehmann and M. Taut, Phys. Status Solidi B **54**, 469 (1972).
[35] M. Balkanski, W. Nazarewicz, and E. Dasilva, in *Lattice Dynamics*, edited by R. F. Wallis (Pergamon, Oxford, 1965), p. 347; M. Balkanski and M. Nusmovici, Phys. Status Solidi **5**, 635 (1964).
[36] G. Dolling, in *Inelastic Scattering of Neutrons in Solids and Liquids*, edited by S. Ekland (IAEA, Vienna, 1963), Vol. II, p. 37.